Room temperature polariton lasing vs. photon lasing in a ZnO-based hybrid microcavity

Tien-Chang Lu,[1,*] Ying-Yu Lai,[1] Yu-Pin Lan,[1] Si-Wei Huang,[1] Jun-Rong Chen,[1] Yung-Chi Wu,[1] Wen-Feng Hsieh,[1] and Hui Deng[2]

[1]*Department of Photonics, National Chiao Tung University, Hsinchu 300, Taiwan*
[2]*Department of Physics, University of Michigan, Ann Arbor, Michigan 48109, USA*
[*] *timtclu@mail.nctu.edu.tw*

Abstract: We report on the room temperature polariton lasing and photon lasing in a ZnO-based hybrid microcavity under optical pumping. A series of experimental studies of the polariton lasing (exciton-photon detunings of $\delta = -119$meV) in the strong-coupling regime are discussed and compared to a photon lasing ($\delta = -45$meV) in the weak-coupling regime obtained in the same structure. The measured threshold power density (31.8kW/cm^2) of polariton lasing is one order of magnitude lower than that of the photon lasing (318.2kW/cm^2). In addition, the comparison between polariton lasing and photon lasing is done in terms of the linewidth broadening, blue-shift of the emission peak, and polarization.

OCIS codes: (140.3945) Microcavities; (140.3948) Microcavity devices.

References and links

1. C. Weisbuch, M. Nishioka, A. Ishikawa, and Y. Arakawa, "Observation of the coupled exciton-photon mode splitting in a semiconductor quantum microcavity," Phys. Rev. Lett. **69**(23), 3314–3317 (1992).
2. H. Den, H. Haug, and Y. Yamamoto, "Exciton-polariton Bose-Einstein condensation," Rev. Mod. Phys. **82**(2), 1489–1537 (2010).
3. H. Deng, G. Weihs, C. Santori, J. Bloch, and Y. Yamamoto, "Condensation of semiconductor microcavity exciton polaritons," Science **298**(5591), 199–202 (2002).
4. J. Kasprzak, M. Richard, S. Kundermann, A. Baas, P. Jeambrun, J. M. J. Keeling, F. M. Marchetti, M. H. Szymańska, R. André, J. L. Staehli, V. Savona, P. B. Littlewood, B. Deveaud, and S. Dang, "Bose-Einstein condensation of exciton polaritons," Nature **443**(7110), 409–414 (2006).
5. R. Balili, V. Hartwell, D. Snoke, L. Pfeiffer, and K. West, "Bose-Einstein condensation of microcavity polaritons in a trap," Science **316**(5827), 1007–1010 (2007).
6. S. Utsunomiya, L. Tian, G. Roumpos, C. W. Lai, N. Kumada, T. Fujisawa, M. Kuwata-Gonokami, A. Löffler, S. Höfling, A. Forchel, and Y. Yamamoto, "Observation of Bogoliubov excitations in exciton-polariton condensates," Nat. Phys. **4**(9), 700–705 (2008).
7. H. Deng, G. Weihs, D. Snoke, J. Bloch, and Y. Yamamoto, "Polariton lasing vs. photon lasing in a semiconductor microcavity," Proc. Natl. Acad. Sci. U.S.A. **100**(26), 15318–15323 (2003).
8. S. Christopoulos, G. B. von Högersthal, A. J. D. Grundy, P. G. Lagoudakis, A. V. Kavokin, J. J. Baumberg, G. Christmann, R. Butté, E. Feltin, J.-F. Carlin, and N. Grandjean, "Room-temperature polariton lasing in semiconductor microcavities," Phys. Rev. Lett. **98**(12), 126405 (2007).
9. G. Christmann, R. Butté, E. Feltin, J.-F. Carlin, and N. Grandjean, "Room temperature polariton lasing in a GaN/AlGaN multiple quantum well microcavity," Appl. Phys. Lett. **93**(5), 051102 (2008).
10. J. J. Baumberg, A. V. Kavokin, S. Christopoulos, A. J. D. Grundy, R. Butté, G. Christmann, D. D. Solnyshkov, G. Malpuech, G. B. von Högersthal, E. Feltin, J.-F. Carlin, and N. Grandjean, "Spontaneous polarization buildup in a room-temperature polariton laser," Phys. Rev. Lett. **101**(13), 136409 (2008).
11. J. Levrat, R. Butté, T. Christian, M. Glauser, E. Feltin, J.-F. Carlin, N. Grandjean, and Y. G. Rubo, "Pinning and depinning of the polarization of exciton-polariton condensates at room temperature," Phys. Rev. Lett. **104**(16), 166402 (2010).
12. J. J. Baumberg, P. G. Savvidis, R. M. Stevenson, A. I. Tartakovskii, M. S. Skolnick, D. M. Whittaker, and J. S. Roberts, "Parametric oscillation in a vertical microcavity: A polariton condensate or micro-optical parametric oscillation," Phys. Rev. B **62**(24), R16247–R16250 (2000).
13. C. Diederichs, J. Tignon, G. Dasbach, C. Ciuti, A. Lemaître, J. Bloch, Ph. Roussignol, and C. Delalande, "Parametric oscillation in vertical triple microcavities," Nature **440**(7086), 904–907 (2006).
14. L. Ferrier, S. Pigeon, E. Wertz, M. Bamba, P. Senellart, I. Sagnes, A. Lemaître, C. Ciuti, and J. Bloch, "Polariton parametric oscillation in a single micropillar cavity," Appl. Phys. Lett. **97**(3), 031105 (2010).
15. K. Davis, M. Mewes, M. Andrews, N. van Druten, D. Durfee, D. Kurn, and W. Ketterle, "Bose-Einstein condensation in a gas of sodium atoms," Phys. Rev. Lett. **75**(22), 3969–3973 (1995).

#158635 - $15.00 USD Received 23 Nov 2011; revised 19 Dec 2011; accepted 10 Jan 2012; published 22 Feb 2012

16. I. R. Sellers, F. Semond, M. Leroux, J. Massies, M. Zamfirescu, F. Stokker-Cheregi, M. Gurioli, A. Vinattieri, M. Colocci, A. Tahraoui, and A. A. Khalifa, "Polariton emission and re□ectivity in GaN microcavities as a function of angle and temperature," Phys. Rev. B **74**(19), 193308 (2006).
17. M. Zamfirescu, A. Kavokin, B. Gil, G. Malpuech, and M. Kaliteevski, "ZnO as a material mostly adapted for the realization of room-temperature polariton lasers," Phys. Rev. B **65**(16), 161205 (2002).
18. J.-R. Chen, T.-C. Lu, Y.-C. Wu, S.-C. Lin, W.-R. Liu, W.-F. Hsieh, C.-C. Kuo, and C.-C. Lee, "Large vacuum Rabi splitting in ZnO-based hybrid microcavities observed at room temperature," Appl. Phys. Lett. **94**(6), 061103 (2009).
19. J.-R. Chen, T.-C. Lu, Y.-C. Wu, S.-C. Lin, W.-F. Hsieh, S.-C. Wang, and H. Deng, "Characteristics of exciton-polaritons in ZnO-based hybrid microcavities," Opt. Express **19**(5), 4101–4112 (2011).
20. S. Kalusniak, S. Sadofev, S. Halm, and F. Henneberger, "Vertical cavity surface emitting laser action of an all monolithic ZnO-based microcavity," Appl. Phys. Lett. **98**(1), 011101 (2011).
21. M. Zamfirescu, A. Kavokin, B. Gil, and G. Malpuech, "ZnO as a material mostly adapted for realization of room-temperature polariton lasers," Phys. Status Solidi **195**(3), 563–567 (2003) (a).
22. S. Faure, T. Guillet, P. Lefebvre, T. Bretagnon, and B. Gil, "Comparison of strong coupling regimes in bulk GaAs, GaN, and ZnO semiconductor microcavities," Phys. Rev. B **78**(23), 235323 (2008).
23. F. Tassone, C. Piermarocchi, V. Savona, A. Quattropani, and P. Schwendimann, "Bottleneck effects in the relaxation and photoluminescence of microcavity polaritons," Phys. Rev. B **56**(12), 7554–7563 (1997).
24. A. I. Tartakovskii, M. Emam-Ismail, R. M. Stevenson, M. S. Skolnick, V. N. Astratov, D. M. Whittaker, J. J. Baumberg, and J. S. Roberts, "Relaxation bottleneck and its suppression in semiconductor microcavities," Phys. Rev. B **62**(4), R2283–R2286 (2000).
25. R. Butté, J. Levrat, G. Christmann, E. Feltin, J.-F. Carlin, and N. Grandjean, "Phase diagram of a polariton laser from cryogenic to room temperature," Phys. Rev. B **80**(23), 233301 (2009).
26. P. G. Lagoudakis, M. D. Martin, J. J. Baumberg, G. Malpuech, and A. Kavokin, "Coexistence of low threshold lasing and strong coupling in microcavities," J. Appl. Phys. **95**(5), 2487 (2004).
27. J. Dai, C. X. Xu, K. Zheng, C. G. Lv, and Y. P. Cui, "Whispering gallery-mode lasing in ZnO microrods at room temperature," Appl. Phys. Lett. **95**(24), 241110 (2009).
28. M. H. Huang, S. Mao, H. Feick, H. Yan, Y. Wu, H. Kind, E. Weber, R. Russo, and P. Yang, "Room-temperature ultraviolet nanowire nanolasers," Science **292**(5523), 1897–1899 (2001).
29. V. M. Markushev, V. V. Ursaki, M. V. Ryzhkov, C. M. Briskina, I. M. Tiginyanu, E. V. Rusu, and A. A. Zakhidov, "ZnO lasing in complex systems with tetrapods," Appl. Phys. B **93**(1), 231–238 (2008).
30. C. Klingshirn, R. Hauschild, J. Fallert, and H. Kalt, "Room-temperature stimulated emission of ZnO: Alternatives to excitonic lasing," Phys. Rev. B **75**(11), 115203 (2007).
31. C. H. Henry, "Theory of the Linewidth of Semiconductor Lasers," IEEE J. Quantum Electron. **18**(2), 259–264 (1982).
32. A. P. D. Love, D. N. Krizhanovskii, D. M. Whittaker, R. Bouchekioua, D. Sanvitto, S. A. Rizeiqi, R. Bradley, M. S. Skolnick, P. R. Eastham, R. André, and S. Dang, "Intrinsic decoherence mechanisms in the microcavity polariton condensate," Phys. Rev. Lett. **101**(6), 067404 (2008).
33. D. M. Whittaker and P. R. Eastham, "Coherence properties of the microcavity polariton condensate," Europhys. Lett. **87**(2), 27002 (2009).
34. H. Haug and S. Koch, "On the Theory of Laser Action in Dense Exciton System," Phys. Status Solidi **82**(2), 531–543 (1977) (b).
35. H. Deng, G. S. Solomon, R. Hey, K. H. Ploog, and Y. Yamamoto, "Spatial coherence of a polariton condensate," Phys. Rev. Lett. **99**(12), 126403 (2007).
36. C. W. Lai, N. Y. Kim, S. Utsunomiya, G. Roumpos, H. Deng, M. D. Fraser, T. Byrnes, P. Recher, N. Kumada, T. Fujisawa, and Y. Yamamoto, "Coherent zero-state and π-state in an exciton-polariton condensate array," Nature **450**(7169), 529–532 (2007).

1. Introduction

Semiconductor microcavities (MCs) are powerful in controlling interaction between light and matter. In a semiconductor MC, strong interaction between excitons and photons would produce new admixed quasiparticles, called exciton-polaritons [1]. Polaritons have a very light effective mass (typically 10^{-8} times the hydrogen atom), have controllable energy-momentum dispersion curves [2], and follow bosonic statistics at low densities. As a result, a wealth of intriguing phenomena and novel applications have been observed and extensively developed in the polariton system, including dynamical polariton Bose-Einstein condensation (BEC) [3–6], polariton lasing [7–11] and polariton parametric oscillator [12–14]. The bosonic nature of polaritons allows them to condense in the state with the lowest kinetic energy. The radiative decay of polaritons from the condensate creates laser-like coherent light, termed polariton lasers. Electronic population inversion is not necessary in such polariton lasers, as compared to conventional lasers, leading to ultra-low threshold coherent light sources. Furthermore, the extremely small effective mass of polaritons enables polariton condensation

#158635 - $15.00 USD Received 23 Nov 2011; revised 19 Dec 2011; accepted 10 Jan 2012; published 22 Feb 2012

at higher critical temperatures compared to atomic system such as Sodium gas (T_c = 2μK) [15], which is crucial for practical applications.

Polariton lasers have been demonstrated in GaAs [3, 7] and CdTe [4] MCs, albeit only at cryogenic temperatures due to the small exciton binding energies in these materials. In contrast, wide-bandgap semiconductor materials have larger exciton binding energies [16], and have emerged as candidates for high temperature polariton lasers. Room temperature (RT) polariton lasing has been demonstrated recently in bulk and multiple-quantum-well (MQW) GaN MCs [8, 9], yet the exciton binding energy in GaN is only comparable to the thermal energy of lattice (k_BT) at 300 K. Another wide-bandgap material, ZnO, possesses even larger oscillator strengths and exciton binding energies (~60 meV in the bulk layer) [17–19]. RT photon lasing in ZnO MCs has been reported very recently [20], but RT ZnO polariton lasers have only been discussed in theory [17, 21]. In this study, we present ZnO polariton lasing at RT under optical pumping and compare the differences of the optical properties between polariton and photon lasers achieved in the same structure at different exciton-photon detunings.

2. Sample structure and experimental details

2.1 Sample structure and fabrication

The hybrid MC structure consists of a bulk ZnO 3λ/2 thick cavity sandwiched between a bottom AlN/$Al_{0.23}Ga_{0.77}N$ distributed Bragg reflector (DBR) with reflectivity of 93% and a top dielectric SiO_2 /HfO_2 DBR with reflectivity of 97%. The 30-pair AlN/AlGaN DBR was grown by metalorganic chemical vapor deposition on a 2.8 μm-thick GaN buffer layer on a c-plane sapphire substrate. The bulk ZnO 3λ/2 thick cavity was grown on the AlN/AlGaN DBR by pulsed-laser deposition. Finally, the 9-period SiO_2 /HfO_2 dielectric DBR was deposited by dual electron-beam gun evaporation to complete the MC structure. The thickness non-uniformity in ZnO cavity and nitride-based DBR provides different exciton-photon detunings.

2.2 Experimental setup

All experiments were performed at RT. A frequency-tripled Nd:YVO_4 355-nm pulse laser with a pulse duration of 0.5 ns and repetition rate of 1 kHz was used as the pumping source. The cavity quality factor Q(= λ/Δλ), based on the measurement of normal incident micro-photoluminescence (μ-PL) system with a pumping spot size of 3 μm focused by a 100x objective lens, was about 221, and the corresponding linewidth and cavity resonance were 15 meV and 3.237 eV, respectively [18]. Two different exciton-photon detunings of δ = –119 meV and δ = –45 meV were investigated in this study and the polariton dispersion curves were measured by the angle-resolved PL system. The laser spot size on the sample surface was about 60 μm in diameter. The emitted light was collected by a UV optical fiber with a 600 μm core mounted on a rotating stage with an angular resolution of 1°, and detected by a nitrogen cooled charge-coupled device attached to a monochromator (iHR 320, HORIBA scientific Inc.) with spectral resolution of about 0.2 nm.

3. Results and discussion

3.1 Dispersion relation of polariton lasing and photon lasing

We show in Fig. 1 the dispersion and momentum space distribution of the emission. Figures 1(a)~1(f) show two dimensional color maps of the RT PL intensity vs. energy and detection angle from the sample normal direction at different excitation powers. Figures 1(g)~1(h) show the integrated intensity of polariton and photon mode for both detunings. Dispersions of the lower polariton branch (LPB) are observed for both detunings at low pumping powers (Figs. 1(a) and 1(d)), which are parabolic-like at small angles and converges to the uncoupled exciton (X) energy at large angles. The small peak energy splitting of LPB observed at large angles (7 meV at 34 degree) in Fig. 1(a) is due to the TE/TM polarizations. The absence of the upper polariton branch (UPB) is expected as a result of the strong absorption in the

#158635 - $15.00 USD Received 23 Nov 2011; revised 19 Dec 2011; accepted 10 Jan 2012; published 22 Feb 2012

scattering and continuum states of ZnO excitons [22] and the polariton thermalization especially in the system with a large normal mode splitting. According to the measured dispersion curves shown in Figs. 1, the estimated Rabi splitting is about 98 meV for large detuning region (δ = –119 meV) and 78 meV for small detuning region (δ = –45 meV) based on the numerical fitting of transfer matrix method. Table 1 shows the different oscillator strength values due to the homogeneous broadening at different pumping power which were considered in the fitting curves of Figs. 1.

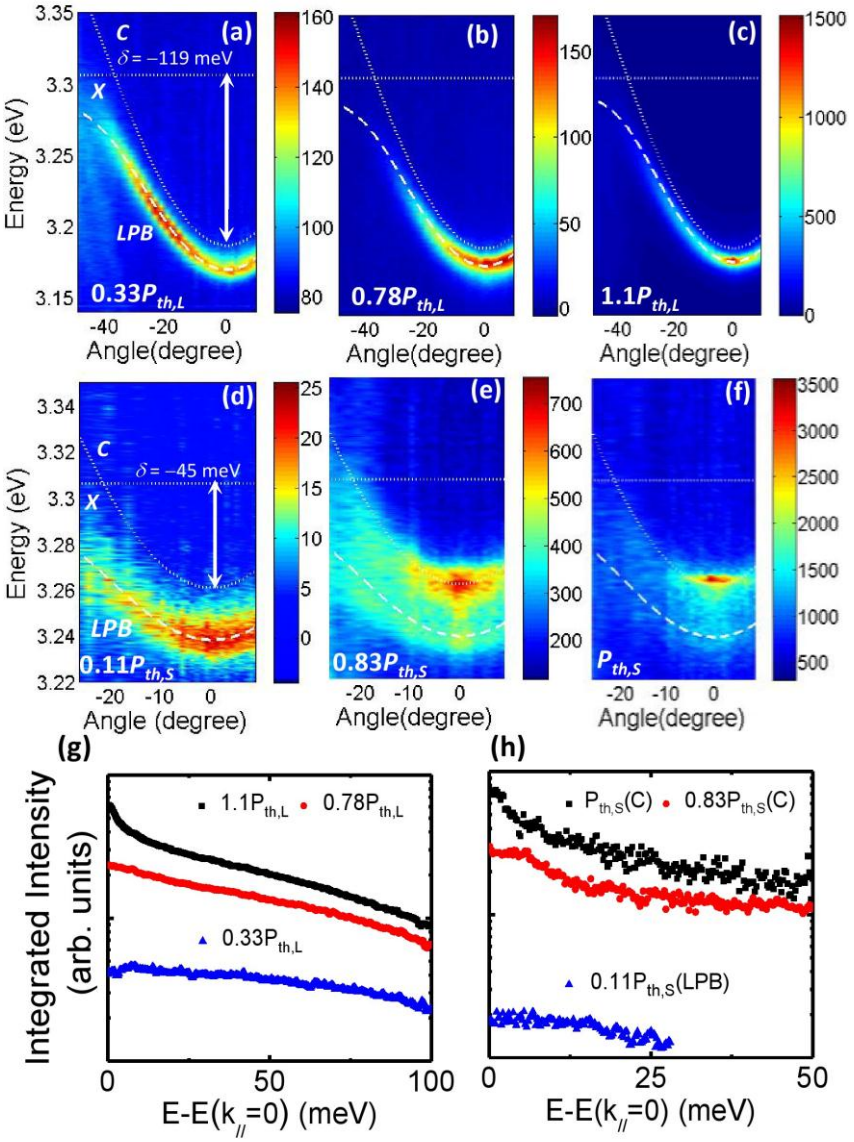

Fig. 1. The color maps of the angular dispersions of measured PL spectra at (a) 0.33$P_{th,L}$, (b) 0.78$P_{th,L}$ and (c) 1.1$P_{th,L}$ for the case of δ = –119 meV (exciton fraction = 11.4%) and (d) 0.11$P_{th,S}$, (e) 0.83$P_{th,S}$, and (f) $P_{th,S}$ for the case of δ = –45 meV (exciton fraction = 25%) at RT. Uncoupled photon mode(C), exciton mode(X) (white dot lines), and LPB (white dash line) are plotted for reference. (g) Integrated intensity of LPB vs energy relative to $E(k_{//} = 0)$ for the case of large detuning. (h) Integrated intensity of LPB (blue spot) and cavity photon mode (red spot and black spot, C) vs energy relative to $E(k_{//} = 0)$ for the case of small detuning.

#158635 - $15.00 USD Received 23 Nov 2011; revised 19 Dec 2011; accepted 10 Jan 2012; published 22 Feb 2012

Table 1. Oscillator strength values in Fig. 1

Large detuning (δ = –119 meV)			Small detuning (δ = –45 meV)		
	Oscillator strength (eV^2)	Power density (kW/cm^2)		Oscillator strength (eV^2)	Power density (kW/cm^2)
Figure 1(a)	0.21	12.7	Figure 1(d)	0.1	42.4
Figure 1(b)	0.14	29.7	Figure 1(e)	0.1	305.6
Figure 1(c)	0.1	42.4	Figure 1(f)	0.1	382.2

In the case of large detuning (δ = –119 meV), at low excitation power density ($0.33P_{th,L}$), a polariton relaxation bottleneck is also observed, as shown in Fig. 1(a). This is because the high photon fraction (88.6%) of lower polariton states resulting in a much shorter lifetime of LPB compared with excitons reduces the probability of hot polaritons to interact with phonons [23, 24]. The polariton relaxation bottleneck is suppressed with increasing pumping power density ($0.78P_{th,L}$), as shown in Fig. 1(b). The integrated polariton intensity follows a Maxwell-Boltzmann distribution, as shown in Fig. 1(g), at a fitted temperature of 324 K. When the pumping power density is larger than threshold ($1.1P_{th,L}$), polariton final state stimulation leads to rapid polariton condensation in the $k_{//} \sim 0$ states, as shown in Fig. 1(c). A peak above the Maxwell Boltzmann distribution is clearly seen near $k_{//} \sim 0$ [Fig. 1(g)].

In the case of small detuning (δ = –45meV), LPB is also observed at low pumping power density, and the relaxation bottleneck is suppressed due to a lower photon fraction (75%) and longer polariton lifetime [23, 24], as shown in Figs. 1(d) and 1(h). However, the higher energy density of states and shallow energy trap of LPB, especially at RT also results in higher threshold power density for polariton final state stimulation scattering, compared with the case of larger negative detuning [25]. Therefore, significant blueshift of the LP energy, accompanied by possibly a transition to the weak-coupling regime, is observed before reaching the threshold $P_{th,S}$. As shown in Fig. 1(e), at $0.83P_{th,S}$ a second emission peak appears and its energy corresponds to the photon mode, indicating the coexistence of pure photon mode and polariton mode emission and the transition from the strong coupling to weak coupling regime. This transition could be firstly induced at the central area of the Gaussian distributed pumping laser spot, and the lower polariton emission could originate from the peripheral area of pumping spot [26]. Above threshold, the photon mode dominates the emission and shows lasing behaviour near the ground state of the photon mode branch [Fig. 1(f)]. The corresponding photon distribution is shown in the k-space [Fig. 1(h)].

3.2 Power dependent characteristics of polariton lasing and photon lasing

The power-dependent emission intensity, linewidth, and emission energy of the polariton and photon lasers are summarized in Figs. 2. For the polariton mode [Figs. 2(a)~2(c)], the lasing threshold power density is $P_{th,L} \sim 31.8$ kW/cm^2, which is much lower than that of the ZnO vertical cavity surface emitting laser (VCSEL) and other low-threshold ZnO nanostructures [20, 27–29]. The corresponding threshold carrier density is $N_{3D} \sim 2.52 \times 10^{17}$ cm^{-3}, which is lower than the Mott density ($3 \times 10^{17} \sim 5 \times 10^{17}$ cm^{-3}) in the bulk ZnO at RT [30]. In general, the emission linewidth of a conventional laser diode under single mode operation decreases with increasing excitation power [31]. The linewidth of polariton mode, on the contrary, narrows at threshold, but then broadens with increasing pumping power, which could be due to the polariton number ñuctuations and self-interactions of polariton in $k_{//} \sim 0$ states as the polariton occupancy in the ground state increases [32, 33]. This phenomenon is evident in Fig. 2(b). In addition, effects of polariton-polariton interaction [34] and oscillator strength saturation of excitons [25] cause a blue-shift of the emission peak energy at $k_{//} \sim 0$ with increasing excitation power [Fig. 2(c)].

For the small detuning case [Figs. 2(d)~2(f)], emission from photon mode appears at $>0.83P_{th,S}$, as marked in the shaded area in Figs. 2(d)~2(f). Further increasing the pump power, photon lasing occurs at the power density of $P_{th,S} \sim 318.2$ kW/cm^2, with the corresponding carrier density of $N_{3D} \sim 2.52 \times 10^{18}$ cm^{-3}. The threshold of the photon lasing is ten times higher than that of the polariton lasing observed in the case of large detuning. The

#158635 - $15.00 USD Received 23 Nov 2011; revised 19 Dec 2011; accepted 10 Jan 2012; published 22 Feb 2012

linewidth of the photon mode narrows significantly at threshold, as shown in Fig. 2(e). Above threshold, the linewidth and the emission peak energy of the photon lasing mode changes negligibly with increasing excitation power, as shown in Figs. 2(e) and 2(f). The linewidth and blue-shift in Figs. 2(e) and 2(f) show a nonlinear tendency when photon mode occurs, indicating the transition from strong coupling to weak coupling regime (marked areas of Figs. 2(e) and 2(f)). This is because, in the weakly coupling regime, lasing takes place in the photon mode whose energy and linewidth are not affected by the exciton's energy and linewidth. These behaviours are in sharp contrast to the polariton lasing and suggest again different origin of the two thresholds.

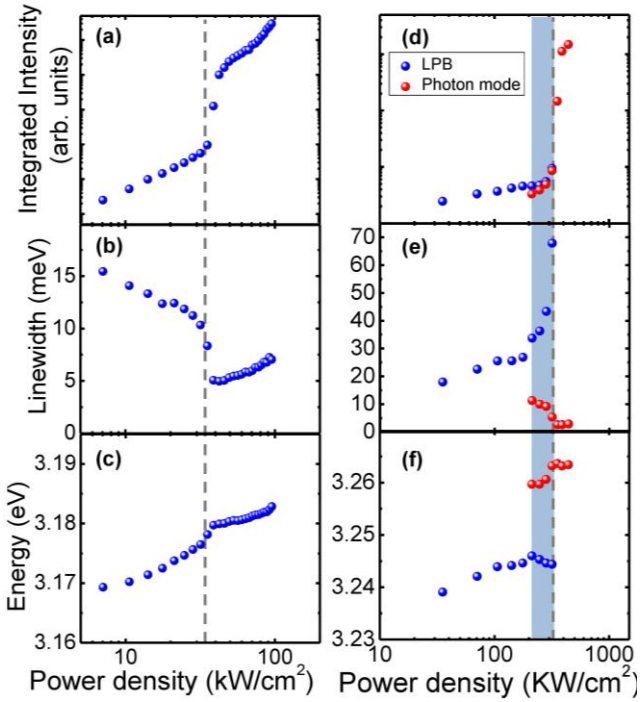

Fig. 2. (a) Integrated emission intensity, (b) emission linewidth and (c) emission energy of polariton versus pump power for the case of large detuning (δ = –119 meV) at RT. (d) Integrated emission intensity, (e) emission linewidth and (f) emission energy of polariton (blue sphere) and photon mode (red sphere) versus pump power for the case of small detuning (δ = –45 meV) at RT.

3.3 Polarization characteristics of polariton lasing and photon lasing

The polariton and photon lasings also feature different polarization properties. Figure 3(a) shows the measured optical polarization for $0.5P_{th,L}$ and $1.7P_{th,L}$ in the case of large detuning. The emission appears to be completely depolarized below and above the threshold. Since the active region is a bulk material, the exciton-exciton scattering should be spin-isotropic. Hence spontaneous polarization occurs with arbitrary polarization direction [10]. On the contrary, the degree of polarization up to 92% as shown in Fig. 3(d) is obtained for the case of small detuning (photon lasing case), indicating that the slight disorder in photonic structure would dominate the polarization characteristics of photon lasing mode. This is consistent with the observation that the energy peak and the lasing linewidth remain the same as the pumping power increases. In addition, the polarization of pumping laser has no relationship to the emission polarization since the pumping is non-resonant.

#158635 - $15.00 USD Received 23 Nov 2011; revised 19 Dec 2011; accepted 10 Jan 2012; published 22 Feb 2012

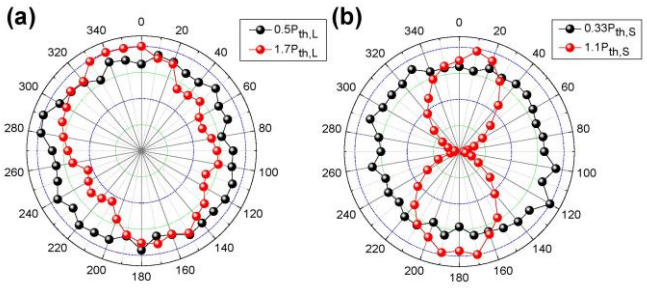

Fig. 3. Polar plots of linear polarization for (a) polariton lasing and (b) photon lasing at above (red sphere) and below (black sphere) threshold condition. The degree of linear polarization up to 92% is obtained in the photon lasing case

3.4 Spontaneous coherence buildup of polariton lasing

Finally, we measure the spatial distribution and spatial coherence of the polariton lasing. Figures 4(a) and 4(b) shows the real space image of LP gas at $0.9P_{th,L}$ and $1.1P_{th,L}$ respectively. Reduction of spatial distribution of LP emission results from the Gaussian profile of the pump spot and large nonlinearity at the threshold [7]. We then pass the spatial image of the LP emission through a Young's double slit to study the spatial coherence [35]. A clear interference pattern appears above threshold, as shown in Figs. 4(c). From the fringe intensity distribution shown in Fig. 4(c), we calculate the first-order degree of coherence $g^{(1)}(r)$ to be about 0.85, at r = 1.5 μm. Compared to the GaAs system, where the coherent length is up to 20 μm at cryogenic temperature [36], our coherent length of polariton lasing in the ZnO MC is limited to 3 μm, which could be due to the larger in-plane spatial disorder or the room temperature operation since the dependence of de Broglie wavelength is inversely proportional to the square root of temperature.

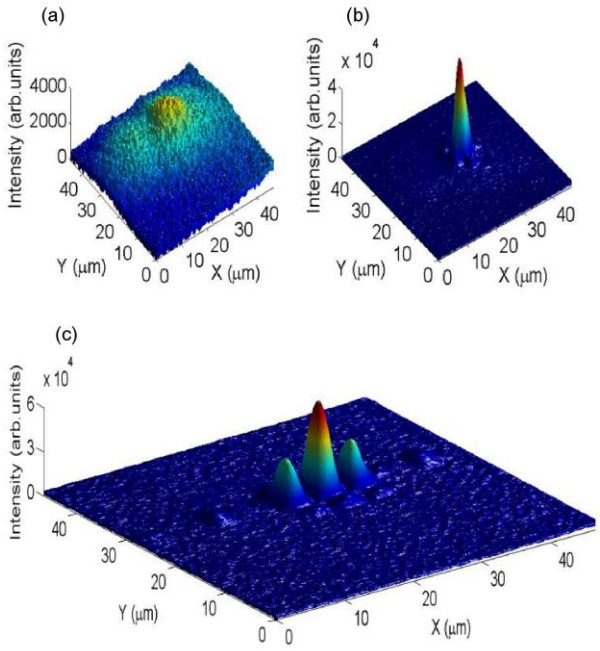

Fig. 4. (a), (b) Spatial distribution of LP at $0.9P_{th,L}$ and $1.1P_{th,L}$. (c) Interference pattern of polariton lasing emission passing through a double-slit at $1.4P_{th,L}$.

#158635 - $15.00 USD Received 23 Nov 2011; revised 19 Dec 2011; accepted 10 Jan 2012; published 22 Feb 2012

4. Conclusion

In conclusion, we have demonstrated RT polariton lasing in a ZnO-based hybrid MC. Characteristics of the polariton lasing have been systematically measured and compared with a photon laser achieved in the same MC at different detunings. The polariton lasing requires a threshold power density (31.8 kW/cm^2) one order of magnitude lower than that of the photon laser (318.2 kW/cm^2). The threshold power density, linewidth broadening, blue-shift of emission peak energy and polarization reveal the fundamental difference between the two types of lasing. The demonstration of ZnO polariton lasing at room temperature promises a novel, ultra-low threshold coherent light source, and facilitates future fundamental research of room temperature quantum degenerate systems and their applications.

Acknowledgments

The authors would like to gratefully acknowledge Prof. Yamamoto at Stanford University for his fruitful suggestion and Prof S. C. Wang and Prof. H. C. Kuo at National Chiao Tung University for technical support. This work has been supported in part by the MOE ATU program and in part by the National Science Council of Republic of China (ROC) in Taiwan under Contract NSC 100-2628-E-009-013-MY3, 99-2221-E-009-035-MY3, and NSC 98-2120-M-009-007.

#158635 - $15.00 USD Received 23 Nov 2011; revised 19 Dec 2011; accepted 10 Jan 2012; published 22 Feb 2012